

Title	Reconstructing carotenoid-based and structural coloration in fossil skin
Authors	McNamara, Maria E.;Orr, Patrick J.;Kearns, Stuart L.;Alcalá, Luis;Anadón, Pere;Peñalver, Enrique
Publication date	2016-03-31
Original Citation	McNamara, M.E., Orr, P.J., Kearns, S.L., Alcalá, L., Anadón, P. and Peñalver, E. (2016) 'Reconstructing carotenoid-based and structural coloration in fossil skin', <i>Current Biology</i> , 26(8), pp. 1075–1082. Available at: https://doi.org/10.1016/j.cub.2016.02.038 .
Type of publication	Article (peer-reviewed)
Link to publisher's version	https://doi.org/10.1016/j.cub.2016.02.038 .
Rights	© 2016 Elsevier Ltd All rights reserved. This manuscript version is made available under the CC-BY-NC-ND 4.0 license. - https://creativecommons.org/licenses/by-nc-nd/4.0/
Download date	2025-04-29 13:42:52
Item downloaded from	https://hdl.handle.net/10468/11873

1 **Reconstructing carotenoid-based and structural coloration in fossil skin**

2 Maria E. McNamara^{1*}, Patrick J. Orr², Stuart L. Kearns³, Luis Alcalá⁴, Pere Anadón⁵ and
3 Enrique Peñalver⁶

4

5 ¹ School of Biological, Earth and Environmental Sciences, University College Cork, Cork,
6 Ireland (maria.mcnamara@ucc.ie)

7 ²UCD School of Earth Sciences, University College Dublin, Belfield, Dublin 4, Ireland
8 (maria.mcnamara@ucc.ie)

9 ³School of Earth Sciences, University of Bristol, Queen's Road, Bristol BS8 1RJ, UK
10 (stuart.kearns@bristol.ac.uk)

11 ⁴Fundación Conjunto Paleontológico de Teruel-Dinópolis, Avda. Sagunto s/n, E-44002 Teruel,
12 Aragón, Spain (alcala@dinopolis.com)

13 ⁵Consejo Superior de Investigaciones Científicas, Institut de Ciències de la Terra 'Jaume
14 Almera', Lluís Solé i Sabarís s/n E-08028, Barcelona, Spain (panadon@ija.csic.es)

15 ⁶Museo Geominero, Instituto Geológico y Minero de España, C/ Ríos Rosas, 23, E-28003,
16 Madrid, Spain (e.penalver@igme.es)

17

18 *Corresponding author. Email: maria.mcnamara@ucc.ie

19

20 Running title: fossil skin colour

21
22
23
24
25
26
27
28
29
30
31
32
33
34
35
36
37
38
39
40
41
42
43

Summary

Evidence of original coloration in fossils provides insights into the visual communication strategies used by ancient animals and the functional evolution of coloration over time [1-7]. Hitherto, all reconstructions of the colours of the plumage of fossil birds and feathered dinosaurs and reptile integument have been of melanin-based coloration [1-6]. Extant animals also use other mechanisms for producing colour [8] but these have not been identified in fossils. Here we report the first examples of carotenoid-based coloration in the fossil record, and of structural coloration in fossil integument. The fossil skin, from a 10 Ma colubrid snake from the Late Miocene Libros Lagerstätte (Teruel, Spain) [9, 10], preserves dermal pigment cells (chromatophores) – xanthophores, iridophores and melanophores – in calcium phosphate. Comparison with chromatophore abundance and position in extant reptiles [11-15] indicates that the fossil snake was pale-coloured in ventral regions; dorsal and lateral regions were green with brown-black and yellow-green transverse blotches. Such coloration most likely functioned in substrate matching and intraspecific signalling. Skin replicated in authigenic minerals is not uncommon in exceptionally preserved fossils [16, 17] and dermal pigment cells generate coloration in numerous reptile, amphibian and fish taxa today [18]. Our discovery thus represents a new means by which to reconstruct the original coloration of exceptionally preserved fossil vertebrates.

Results

44 The integument of vertebrates is a complex system with important functions in homeostasis,
45 sensory reception and, via its coloration, visual signaling [18]. Recent studies have reconstructed
46 the melanin-based [2-6] plumage colours of feathered dinosaurs and birds on the basis of
47 preserved melanosomes [2-5] and feather chemistry as revealed by X-ray mapping [6]. Melanin-
48 based pigmentation, however, is only one of several pigment-based mechanisms for producing
49 colour [18]; evidence of other pigments has not been reported in fossil vertebrates. Examples of
50 fossilized vertebrate skin are not uncommon and have yielded insights into the biology [19-23]
51 of non-feathered dinosaurs and other fossil reptiles, but evidence of original coloration and
52 patterning in fossil skin has, until now, been limited to rare instances of subtle monotonal
53 patterning [5, 19]. Here we report the discovery of intact dermal chromatophores, the pigment
54 cells responsible for coloration and patterning, in a 10 million year old colubrid snake. We use
55 scanning electron microscopy to analyze the relative abundance and vertical position of the
56 chromatophores from different body regions. By comparing these data to those from extant
57 snakes, we reconstruct the original integumentary colour patterns of the fossil snake and reveal
58 their ecological functions.

59

60 The fossil snake (Museo Nacional de Ciencias Naturales (CSIC) MNCN 66503) occurs within
61 Vallesian (11.2–8.7 Ma) oil shales of the Libros Gypsum lacustrine sequence [9, 24], which
62 outcrops 25 km SE of Teruel city, NE Spain (40°07'38"N 1°12'1"W). The specimen was
63 recovered during mining operations in the early 20th century; stratigraphic data are not available.
64 It is in lateral aspect and lacks a cranium (Figure 1A), and is assigned to the Colubridae. A more
65 precise taxonomic determination is not possible in the absence of a cranium. The specimen is on
66 permanent display at Dinópolis palaeontological museum in Teruel, Spain.

67

68 **Ultrastructure and chemistry of the fossil snake skin**

69 The fossil skin extends from the vertebrae to the ventral termini of the ribs (Figures 1A, 1B);
70 overlapping scales are evident (Figure 1B). Scanning electron microscopy reveals that the fossil
71 skin, as with many fossilized decay-prone tissues [25], is replicated in calcium phosphate. It
72 exhibits a tripartite division into a thin (6–9 μm thick) outer layer that is structureless and
73 nanocrystalline, a thicker (15–25 μm thick) central layer that contains mineralized fibres and
74 oblate to spheroidal bodies, and a thick (100–180 μm) lowermost layer that comprises a
75 plywood-like array of fibres (Figures 1C, 1D). These fossil skin layers correspond to the main
76 layers of the skin in extant reptiles [8, 18], i.e. the epidermis (comprised of keratinized cells),
77 upper dermal stratum spongiosum (loosely packed collagen fibres and chromatophores (pigment
78 cells)) and lower dermal stratum compactum (a dense orthogonal array of collagen fibres). The
79 stratum compactum in the fossil snake is locally underlain by a thin (8–13 μm thick) structureless
80 layer (Figure 1C) that represents the remains of the basement membrane which in extant reptiles
81 separates the skin from the underlying hypodermis [8, 18].

82

83 The most striking features of the stratum spongiosum in the fossil snake skin are abundant oblate
84 to spheroidal bodies, consistently located immediately below the epidermal-dermal boundary
85 (Figures 1D–K; Figure 2). These bodies fall into three types that are differentiated on their
86 location, size, morphology and internal fill.

87

88 Type 1 bodies occur at the top of the array; they are small (1–5 μm x 0.4–2 μm) cryptocrystalline
89 discs (Figures 1E, 1F) that can be organized into a layer up to four discs thick (Figures 2C, 2H,

90 2I, Figures S1E–H). As with other features of the skin, the discs are frequently separated from
91 the surrounding matrix by a void (Figure 1F).

92

93 These discs are underlain by Type 2 bodies, which are larger (3–8 μm long) irregular spheroids
94 to ovoids that comprise granules of two types: small (0.15–0.4 μm) subspherical granules with
95 irregular to rounded outlines, and larger (0.8–1.2 μm) rounded granules with smooth outlines
96 (Figures 1G, 1J). The relative proportions of the two granule types are similar and consistent
97 among the Type 2 bodies (smaller vesicles: $44.2 \pm 4.7\%$; $n = 38$).

98

99 The Type 2 bodies are underlain by larger (8–20 μm long) ovoid features with smooth outlines,
100 and prominent lateral processes. These Type 3 bodies contain densely packed granules with a
101 narrow size distribution (0.18–0.3 μm) (Figures 1H, 1I, 1K).

102

103 Elemental mapping of the fossil snake skin reveals that the bodies in the stratum spongiosum and
104 dermal collagen fibres contain elevated concentrations of S, and lower concentrations of C and P,
105 relative to other ultrastructures in the skin (Figure 3). No other elements show spatial partitioning
106 among the various structures in the skin.

107

108 **Discussion**

109 **Interpretation of the bodies as fossil chromatophores**

110 The bodies preserved in the stratum spongiosum of the fossil snake are unlikely to be skin
111 glands: in extant snakes, skin glands are restricted to a pair of anal scent glands [18]. Similarly,
112 there is no evidence that the bodies (or their internal granular fill) represent fossilized decay

113 bacteria [see 26]. The disc-like morphology of the Type 1 bodies is not consistent with that of
114 bacteria. The Type 2 and 3 bodies are too large to represent bacteria, which are usually 0.5–2 μm
115 long [27]. Fossil bacteria would be expected to infest the entire tissue during decay (including
116 the dermis), not just specific features such as the interior of the chromatophores. Bacteria could
117 also generate a characteristic texture whereby they pseudomorph the gross geometry of the
118 original tissue; if replicated in calcium phosphate this is termed a microbial microfabric [28].
119 Further, preserved bacteria are not associated with other fossils from Libros: recent geochemical
120 analyses reveal that microbe-like microstructures associated with fossil amphibians from Libros
121 can be convincingly identified as preserved melanosomes [29]. The bodies preserved within the
122 uppermost stratum spongiosum of the fossil snake skin are therefore interpreted as fossil
123 chromatophores, which are common components of the upper stratum spongiosum in extant
124 snakes [18]; the three types of body are interpreted as three different chromatophore types. The
125 skin of the Libros snake is thus preserved as a substrate microfabric [28] whereby
126 nanocrystalline calcium phosphate has faithfully replicated the ultrastructure of the tissue.

127
128 Certain pigments, including melanins, pteridines and carotenoids are known to have an affinity
129 for metal cations [30-32]. Elevated levels of sulfur in the dermal chromatophores and collagen
130 fibres may reflect the presence of sulfur-bearing moieties in the original tissue structures [33, 34]
131 or the incorporation of sulfur (in the form of sulfate) into the replacement phosphate during
132 mineralization [35]. There is no evidence, however, for partitioning of trace elements among the
133 various chromatophores in the fossil snake skin (Figure 3). This may reflect concentrations
134 below detection limits (< 100 ppm) or overprinting of the original trace element chemistry during
135 the mineralization process. The fossil chromatophores are therefore interpreted on the basis of

136 their size, geometry and, in some examples, internal structure compared with those in extant
137 reptiles [8, 11-15] (Figures 1E-K, Figures S1-S5). Some of the chromatophores in the fossil skin
138 are present as external moulds; their affinities are resolved by their shape and study (at high
139 magnification) of the surface texture of the mould (see insets in Figure S1D).

140

141 In extant reptiles, dermal melanophores are readily identified by their position at the base of the
142 chromatophore array, their large size (10–30 μm wide), prominent lateral processes, and infill of
143 small granules of melanin (melanosomes) with a narrow size distribution [8, 12]. Dermal
144 melanophores typically exhibit ovoid geometries when in the contracted state (whereby
145 melanosomes are restricted to the main body of the melanophore [36]) and have few lateral
146 processes [36] and a low packing density (Figure 1 in [12], Figure 7 in [36], Figure 8 in [37]).
147 The melanosomes vary in size among modern taxa (0.15–0.8 μm long x 0.25–0.5 μm wide) but
148 for a given taxon have a small size range (Figure 2a in [11], Figure 1 in [12], Figure 3 in [13],
149 Figure 7 in [14], Figure 1 in [15], Figure 1 in [35], Figure 5 in [37]). The Type 3 bodies in the
150 fossil snake skin share all the main characteristics of, and are thus best interpreted as, dermal
151 melanophores.

152

153 Iridophores are small chromatophores (usually 5–10 μm wide [12, 14, 18]) that have irregular to
154 flattened or disc-like morphologies. They can form vertical stacks up to four cells thick [12] and
155 can occur at the top of the chromatophore array [11, 12] or below an upper layer of xanthophores
156 [12, 14, 15]. The Type 1 bodies in the fossil snake also have a flattened geometry and occur in
157 stacks in some body regions; these features are consistent with an interpretation as iridophores
158 but not as any other ultrastructural feature of the skin. The small size of the fossil iridophores (1–

159 5 μm) may reflect taxonomic factors (as with melanophores, above) or degradation during the
160 fossilization process. In extant reptiles, iridophores contain angular crystalline platelets of the
161 purines guanine, hypoxanthine or adenine [18]. These platelets are not preserved in the fossil
162 snake, but this is not unexpected: guanine is soluble in dilute acids [38], which are typical
163 products of decay [25].

164
165 Xanthophores in extant snakes are typically 3–10 μm long and have irregular to spheroidal or
166 ovoid geometries [12, 18]. They have been defined as chromatophores that contain abundant
167 granules of carotenoids and pteridines [12, 18]; others differentiate between primarily
168 carotenoid-bearing xanthophores, and primarily pteridine-bearing erythrophores [12, 18]. The
169 former definition is used herein. Granules of pteridines – pterinosomes – are vesicles (0.3–1 μm)
170 with a smooth rounded surface, spherical to elongate geometry and internal concentric laminae
171 [13] (Figure 2A in [11], Figure 10 in [12], Figure 10 in [14], Figure 5 in [37], Figure 4 in [39]).
172 Carotenoid granules are smaller (0.15–0.45 μm) and have smooth (Figure 1 in [36]) or irregular
173 (Figure 2 in [12]) outlines, i.e. subrounded to angular geometries [12]. The Type 2 bodies in the
174 fossil snake occur below the iridophores and above the melanophores, and have irregular
175 spheroidal to ovoid outlines. The internal granules fall into two discrete types: small subspherical
176 granules with irregular outlines, and larger rounded granules with smooth outlines; these most
177 likely correspond to fossil carotenoid and pterinosome vesicles, respectively. The similar
178 proportions of the two granule types in the Type 2 bodies is not consistent with an interpretation
179 as erythrophores [12]. The most parsimonious interpretation is therefore that the irregular
180 spheroidal to ovoid chromatophores in the fossil snake represent xanthophores filled with a
181 combination of large pterinosomes and smaller carotenoid granules.

182

183 **Relating chromatophores to visible hue**

184 In extant reptiles, the visible hue of the integument is produced by a combination of dermal
185 chromatophores, epidermal melanocytes and epidermal diffraction gratings. In the fossil snake,
186 the epidermis is poorly preserved and thus the former presence of epidermal melanocytes and
187 surficial diffraction gratings cannot be determined. The contribution of these features to visible
188 hue and patterning, however, would have been minimal [12, 18, 36, 40]. Epidermal melanocytes
189 are not involved in creating colour patterning [12, 18]; they typically occur only in skin regions
190 of dark brown to black hue, enhancing the effect of a thick dense layer of dermal melanophores
191 [41]. Epidermal diffraction gratings generate weak spectral iridescence that is superimposed on
192 colour patterns generated by dermal chromatophores, which are the primary contributors to
193 visible hue [40].

194

195 Our interpretation of the original colour of the fossil snake is therefore based entirely on the
196 dermal chromatophores. Samples of skin from different body regions of the fossil snake exhibit
197 systematic differences in the type, and relative abundance, of chromatophores (Figures 1C, 2,
198 Figures S1-S5; Table S1); these differences are statistically significant ($\chi^2 = 42.6$; $df = 3, 5$; $\chi^2_8 =$
199 20.09 , $p < 0.01$). There is no evidence that this variation reflects taphonomic factors. The fidelity
200 of preservation of the chromatophores does not vary with chromatophore abundance, i.e. the
201 chromatophores are equally well preserved (in terms of definition of external margins and nature
202 of internal fill) where rare and abundant (compare Figures 2A and 2F). Further, the overall
203 fidelity of preservation of the skin does not vary among different body regions, e.g. collagen
204 fibres are preserved with equal fidelity throughout. There is thus no evidence that certain regions

205 of the skin were subjected to more extensive decay than others and that the preserved abundance
206 of melanosomes is a taphonomic artefact.

207
208 Synthesis of published literature on reptile chromatophores (Table S2) and primary observations
209 (Figure S4) reveal that in extant reptiles, specific combinations of chromatophores correspond to
210 different hues (Table S2). The colours of the fossil snake can thus be reconstructed based on the
211 relative abundance and stratigraphy of the chromatophores. In extant reptiles, iridophores scatter
212 light from crystals of guanine and other purines through thin film interference [8]. Xanthophores
213 are capable of producing a range of yellow, orange and red hues, depending on the relative
214 proportions of carotenoid granules and pterinosomes present [12, 18]. Xanthophores with equal
215 amounts of both granule types – as in the fossils – produce yellowish hues [12]. Melanophores
216 produce brown to black hues as their melanosomes absorb most, or all, wavelengths of light [12].

217
218 Samples 1, 2, 3, 5 and 7 are from lateral body regions; 4 is dorsal, and 6, ventral. Patterning in
219 snakes is typically repeated along the length of the body [8] and thus our colour reconstruction,
220 based on comprehensive sampling of one body region, can be extrapolated to the remainder.

221 There is no evidence that the fossil snake skin exhibited white, red, blue, or grey hues. All skin
222 regions studied preserve chromatophores, eliminating the possibility of white hues [12]. There is
223 no evidence that any xanthophores comprised primarily pterinosomes, eliminating the possibility
224 of red hues [12, 18, 41]. No skin regions exhibited only iridophores and melanophores,
225 eliminating the possibility of structural blue [11], structural green (Figure S4) and grey hues.

226 Iridophores can reflect specific, or all, visible wavelengths depending on the thickness and

227 organization of the internal purine platelets [8]. Given that the latter are not preserved in the
228 fossils, we cannot comment on their potential contribution to the original colour.

229

230 Iridophores and xanthophores are abundant and melanophores common in two samples from
231 lateral body regions (samples 5 (Figure 1E) and 7 (Figures 2A, S2)). In extant reptiles, similar
232 chromatophore architectures (in particular, the presence of carotenoid-bearing xanthophores and
233 the position of iridophores at the top of the chromatophore array) are associated with green hues
234 [11]. In other lateral body regions (sample 2) melanophores are more abundant and iridophores
235 and xanthophores, less abundant (Figures 2B, S2), suggesting darker, less saturated green hues.
236 Skin samples from other lateral body regions (sample 1) exhibit stacks of iridophores up to four
237 cells thick (Figure 2C), indicating brighter green hues: layering of iridophores markedly
238 increases integument albedo [42]. Conversely, other lateral regions (sample 3) exhibit abundant
239 melanophores; xanthophores are common and iridophores, rare to absent (Figure 2D, S3),
240 characteristic of dark brown/black tones [11]. In dorsal regions (sample 4) xanthophores are
241 abundant, iridophores, common and melanophores, rare (Figures 2E, S3), indicating yellowish to
242 pale brown hues [18]. In ventral regions (sample 6), iridophores and xanthophores are abundant,
243 and melanophores, rare to absent (Figures 2F, S1), corresponding to cream-coloured hues [40].

244

245 The fossil snake can therefore be reconstructed as green with brown/black blotches on its dorsal
246 and lateral surfaces, and pale ventrally (Figure 4). Similar coloration characterizes some extant
247 Colubrid snakes, e.g. *Nerodia floridana* and *Dispholidus typus*.

248

249 **Broader implications**

250 Green coloration is an effective adaptation for substrate matching in foliage [43]. This cryptic
251 visual signal was enhanced by two pattern elements. The superimposition of brown/black tones
252 on the green background formed a disruptive pattern to conceal the body contours [43].
253 Countershading via dark and light colours on dorsal and ventral surfaces, respectively, decreases
254 apparent relief [44]. Complex patterning indicates a diurnal lifestyle and strong selection for
255 substrate matching to reduce visibility to visual predators [45]. Patterning in extant reptiles often
256 comprises a mosaic of elements reflecting antagonistic selective pressures relating to
257 homeostasis and signalling [11]. Bright hues may impact negatively on survival but are
258 implicated in social interactions [46]. Thus the patterning in the fossil snake probably served
259 dual functions in camouflage and intraspecific signalling.

260
261 Until now, reconstructions of the original coloration of fossil vertebrates have been of melanin-
262 based mechanisms and from soft tissues preserved as carbonaceous remains. Reconstructions of
263 the original colours of vertebrates preserved via this pathway have not been able to incorporate
264 contributions from non-melanin-based coloration mechanisms [3]. Maturation experiments
265 simulating aspects of the organic preservation process have shown that non-melanin-based
266 coloration mechanisms have a lower preservation potential than those that are based on melanin
267 [47]. Our discovery confirms that direct evidence for diverse coloration mechanisms can be
268 preserved in fossils preserved via an alternative preservation pathway, namely replication of
269 tissues in authigenic minerals, and that the high fidelity of preservation allows original coloration
270 to be reconstructed. The various factors that control phosphatization of soft tissues are known
271 [25] and fossil examples of phosphatized skin are not uncommon; importantly, they have been
272 reported from various taxa and fossil localities [16, 17], suggesting that our discovery has broad

273 applications in the fossil record. Our discovery should prompt a search for other examples, and is
274 likely to be the first example of a recurrent phenomenon. Integuments replicated in calcium
275 phosphate are obvious targets for further attempts to reconstruct colour patterns derived from
276 melanin and, critically, other pigments and structural coloration mechanisms, across diverse
277 vertebrate groups.

278

279 **Experimental Procedures**

280 **Electron microscopy**

281 Samples of fossilised skin were prepared for scanning and transmission electron microscopy as
282 in [7]. Samples of skin from the extant snake *Ahaetulla prasina* were frozen with liquid N₂ and
283 fractured with a scalpel. Samples were examined using a FEI XL-30 ESEM-FEG SEM, a FEI
284 Quanta 650 FEG SEM and a Hitachi S-3500N variable pressure SEM at accelerating voltages of
285 5–15kV and a JEOL 2100 TEM at an accelerating voltage of 200 kV.

286

287 **Electron probe microanalysis**

288 Samples of fossilised skin were embedded in resin, polished, and examined using a JEOL JXA
289 8530F Electron Microprobe. All maps were produced in wavelength dispersive X-ray
290 spectroscopy mode at an accelerating voltage of 15 kV, current of 10 nA and dwell time of 500
291 ms per pixel.

292

293

294 **Histology**

295 Samples of skin from the extant snakes *Ahaetulla prasina*, *Crotalus scutulatus* and *Thamnophis*
296 *sirtalis* were fixed and dehydrated as in [7] and embedded in paraffin wax. 30 µm thick sections
297 were stained using haematoxylin and eosin.

298

299 **Author contributions**

300 MMN designed the study and wrote the manuscript with input from all other authors. SK carried
301 out EPMA analyses, and MMN, all other analyses.

302

303 **Acknowledgments**

304 We thank Daniel Ayala, Eduardo Espílez, Sharon Lynch, Zhenting Jiang, Twan Leenders,
305 Patricia Pérez, Begoña Sánchez, Joe Tobin, Greg Watkins-Colwell. The research was funded by
306 Enterprise Ireland Basic Research Grant C/2002/138 awarded to PJO and by an IRCSET-Marie
307 Curie International Mobility Fellowship and a Marie Curie Career Integration Grant awarded to
308 MEM. The authors declare no conflicts of interest.

309

310 **Data Accessibility**

311 Data are available at the Cork Open Research Archive (CORA) (<http://cora.ucc.ie>). Requests for
312 specimens and samples should be addressed to MMN.

313

314 **References**

- 315 1. Carney, R., Vinther, J., Shawkey, M., D'Alba, L., and Ackermann, J. (2011). New
316 evidence on the colour and nature of the isolated *Archaeopteryx* feather. *Nature Comm.*
317 *3*, 637–643.
- 318 2. Zhang, F., Kearns, S., Orr, P.J., Benton, M., Zhou, Z., Johnson, D., Xu, X., and Wang, X.
319 (2010). Fossilized melanosomes and the colour of Cretaceous dinosaurs and birds. *Nature*
320 *463*, 1075–1078.
- 321 3. Li, Q., Gao, K., Vinther, J., Shawkey, M., Clarke, J., D'Alba, L., Meng, Q., Briggs, D.,
322 and Prum, R. (2010). Plumage color patterns of an extinct dinosaur. *Science* *327*, 1369–
323 1372.
- 324 4. Li, Q., Clarke, J.A., Gao, K.-Q., Zhou, C.-F., Li, D., D'Alba, L. and Shawkey, M.D.
325 (2014). Melanosome evolution indicates a key physiological shift within feathered
326 dinosaurs. *Nature* *507*, 350–353.
- 327 5. Lindgren, J., Sjövall, P., Carney, R., Uvdal, P., Gren, J., Dyke, G, Schultz, B., Shawkey,
328 M., Barnes, K., and Polcyn, M. (2014). Skin pigmentation provides evidence of
329 convergent melanism in extinct marine reptiles. *Nature* *506*, 484–486.
- 330 6. Wogelius, R. *et al.* (2011). Trace metals as biomarkers for eumelanin pigment in the
331 fossil record. *Science* *333*, 1622–1626.
- 332 7. McNamara, M.E., Briggs, D.E.G., Orr, P.J., Wedmann, S., Noh, H., and Cao, H. (2011).
333 Fossilized biophotonic nanostructures reveal the original colors of 47-million-year-old
334 moths. *PLoS Biol.* *9*, e1001200.
- 335 8. Cooper, W., and Greenberg, N. (1992). Reptilian Coloration and Behaviour. In *Biology*
336 *of the Reptilia: Physiology*, E. C. Gans , and D. Crews, eds. (Chicago: University of
337 Chicago Press), pp. 298–422.

- 338 9. Ortí, F., Rosell, L., and Anadón, P. (2003). Deep to shallow lacustrine evaporites in the
339 Libros gypsum (southern Teruel Basin, Miocene, NE Spain): an occurrence of pelletal
340 gypsum rhythmites. *Sedimentology* 50, 361–386.
- 341 10. Navás, L. 1922 Algunos fósiles de Libros (Teruel). *Bol. Soc. Ibér. Cien. Nat.* 21, 52–61.
- 342 11. Kuriyama, T., Sugimoto, M., and Hasegawa, M. (2006). Ultrastructure of the dermal
343 chromatophores in a lizard (Scincidae: *Plestiodon latiscutatus*) with conspicuous body
344 and tail coloration. *Zool. Sci.* 23, 793–799.
- 345 12. Alexander, N., and Fahrenbach, W. (1969). The dermal chromatophores of *Anolis*
346 *carolinensis* (Reptilia: Iguanidae). *Am. J. Anat.* 126, 41–56.
- 347 13. Miscalencu, D., and Ionescu, M.D. (1973). The fine structure of the epidermis and dermal
348 chromatophores in *Vipera ammodytes*. *Acta Anat.* 86, 111–122.
- 349 14. Breathnach, A.E., and Poyntz, S.V. (1966). Electron microscopy of pigment cells in tail
350 skin of *Lacerta vivipara*. *J. Anat.* 100, 549–569.
- 351 15. Morrison, R.L., Rand, M.S., and Frost-Mason, S.K. (1995). Cellular basis of color
352 differences in three morphs of the lizard *Sceloporus undulatus*. *Copeia* 2, 397–408.
- 353 16. Martill, D.M., and Unwin, D. (1989). Exceptionally well preserved pterosaur wing
354 membrane from the Cretaceous of Brazil. *Nature* 340, 138–140.
- 355 17. Martill, D.M., Batten, D.J., and Loydell, D.K. (2000). A new specimen of the
356 thyreophoran dinosaur cf. *Scelidosaurus* with soft tissue preservation. *Palaeontol.* 43,
357 549–559.
- 358 18. Landmann, L. (1986). Epidermis and Dermis. In *Biology of the integument*, J. Bereiter-
359 Hahn, A. Matoltsy, and K. Sylvia-Richards, eds. (Berlin: Springer), pp. 150–187.

- 360 19. Lingham Soliar, T., and Plodowski, G. (2010). The integument of *Psittacosaurus* from
361 Liaoning Province, China: taphonomy, epidermal patterns and color of a ceratopsian
362 dinosaur. *Naturwissenschaften* 97, 479–486.
- 363 20. Lindgren, J., Alwmark, C., Caldwell, M.W., and Fiorillo, A.R. (2009). Skin of the
364 Cretaceous mosasaur *Plotosaurus*: implications for aquatic adaptations in giant marine
365 reptiles. *Biol. Lett.* 5, 528–531.
- 366 21. Czerkas, S.A. (1997). Skin. In *Encyclopedia of dinosaurs*, P.J. Currie, and K. Padian, eds.
367 (San Diego: Academic Press), pp. 669–675.
- 368 22. Horner, J. (1984). A 'segmented' epidermal tail frill in a species of hadrosaurian dinosaur.
369 *J. Paleontol.* 5, 270–271.
- 370 23. Manning, P.L. *et al.*, (2009). Mineralized soft-tissue structure and chemistry in a
371 mummified hadrosaur from the Hell Creek Formation, North Dakota (USA). *Proc. R.*
372 *Soc. B* 276, 3429–3437.
- 373 24. Anadón, P., Cabrera, L., Julià, R., Roca, E., and Rosell, L. (1989). Lacustrine oil-shale
374 basins in Tertiary grabens from NE Spain (Western European Rift System). *Palaeogeogr.,*
375 *Palaeoclimatol., Palaeoecol.* 70, 7–28.
- 376 25. Briggs, D.E.G. (2003). The role of decay and mineralisation in the preservation of soft-
377 bodied fossils: *Ann. Rev. Earth Planet. Sci.* 31, 275–301.
- 378 26. Moyer, A., Zheng, Q., Johnson, E.A., Lamanna, M.C., Li, D., Lacovara, K.J., and
379 Schweitzer, M.H. (2014). Melanosomes or microbodies: testing an alternative hypothesis
380 for the origin of microbodies in fossil feathers. *Sci. Rep.* 4, 4233.
- 381 27. Liebig, K. (2001). Bacteria. In *Palaeobiology II*, D.E.G. Briggs, and P. Crowther, eds.
382 (Oxford, Blackwell), pp. 253–256.

- 383 28. Wilby, P.R., and Briggs, D.E.G. (1997). Taxonomic trends in the resolution of detail
384 preserved in fossil phosphatized soft tissues. *Geobios Mém. Spéc.* 20, 493–502.
- 385 29. McNamara, M.E., van Dongen, B., Bull, I., and Orr, P.J., Fossilisation of melanosomes
386 via sulphurisation, *Palaeontology* (accepted).
- 387 30. Simon, J.D., Peles, D., Wakamatsu, K., and Ito, S. (2009). Current challenges in
388 understanding melanogenesis: Bridging chemistry, biological control, morphology, and
389 function. *Pigment Cell Melanoma Res.* 22, 563–579.
- 390 31. Albert, A. (1953). Quantitative studies of the avidity of natural substances for trace
391 metals: 3. Pteridines, riboflavin and purines. *Biochem. J.* 54, 646–654.
- 392 32. Burgmayer, S.J., and Stiefel, E.I. (1988). Reactions of molybdate with dithiothreitol.
393 Structure of [TEA]₂[Mo₂O₅dt]. *Inorg. Chem.* 27, 4059–4065.
- 394 33. Hames, D., and Hooper, N. (2011). *Biochemistry* (Oxford, Taylor and Francis).
- 395 34. Tscheche, R. (1954). The constitution of urothione. In *Biology and Chemistry of*
396 *Pteridines*. G.E.W. Wolstenholme, and M.P. Cameron, eds. (Boston, Little, Brown &
397 Co.), pp. 135–139.
- 398 35. Poulton, S.W., Bottrell, S.H., and Underwood, C.J. (1998). Porewater sulphur
399 geochemistry and fossil preservation during phosphate diagenesis in a Lower Cretaceous
400 shelf mudstone. *Sedimentology* 45, 875–887.
- 401 36. Bagnara, J.T., Taylor, J.D., and Hadley, M.E. (1968). The dermal chromatophore unit. *J.*
402 *Cell. Biol.* 38, 67–79.
- 403 37. Taylor, J.D., and Hadley, E.M. (1970). Chromatophores and colour change in the lizard
404 *Anolis carolinensis*. *Zeitschr. Zellforschung.* 104, 282–294.

- 405 38. Nelson, D., and Cox, M. (2008). *Lehninger Principles of Biochemistry*, Fifth Edition
406 (New York: Freeman).
- 407 39. Gregory, C.R., Harmon, B.G., Latimer, K.S., Hafner, S., Campagnoli, R.P.,
408 MacManamon, R.M., and Steffens, R.L. (1997). Malignant chromatophoroma in a
409 canebrake rattlesnake (*Crotalus horridus atricaudatus*). *J. Zoo. Wildl. Med.* 28, 198–203.
- 410 40. Bechtel, H.B. (1978). Color and pattern in snakes (Reptilia, Serpentes). *J. Herpetol.* 12,
411 521–532.
- 412 41. Bechtel, H.B. (1995). *Reptile and amphibian variants: colors, patterns, and scales*
413 (Malabar: Krieger).
- 414 42. Kleese, W. (1981). Dermal iridophores in snakes, PhD thesis, University of Arizona.
- 415 43. Hadley, M. (1972). Functional significance of vertebrate integumental pigmentation.
416 *Amer. Zool.* 12, 63–76.
- 417 44. Rowland, H. (2009). From Abbott Thayer to the present day: what have we learned about
418 the function of countershading? *Proc. R. Soc. Lond. B* 364, 519–527.
- 419 45. Kettlewell, B. (1973). *The evolution of melanism: the study of a recurring necessity*
420 (Oxford: Clarendon Press).
- 421 46. Carretero, M. (2002). Sources of colour pattern variation in Mediterranean
422 *Psammodromus algirus*. *Neth. J. Zool.* 52, 43–60.
- 423 47. McNamara M.E., Briggs D.E.G., Orr P.J., Field, D., and Wang, Z. (2013). Experimental
424 maturation of feathers: implications for reconstructions of fossil feather colour. *Biology*
425 *Letters* 9, 20130184.

426

427 **Figure legends**

428 Figure 1. Preserved skin in a fossil colubrid snake (MNCN 66503). (A) Entire specimen; inset,
429 anterior. Cream-coloured material is fossil skin. Numerals 1–7 indicate sample locations. (B)
430 Overlapping scales. (C–E) Scanning electron micrographs (SEMs) of fractured vertical sections
431 through the skin, showing epidermis (Epi), dermis (De), basement membrane (B),
432 chromatophores (iridophores (I), melanophores (M), xanthophores (X)), stratum spongiosum
433 (Sp), stratum compactum (Sc), and collagen fibres (C). (F–I) Details of iridophore (F),
434 xanthophore (G), melanophores (H, I). (J, K) Transmission electron micrographs of xanthophore
435 (J), melanophore (K). The voids in SEM images typically represent structures that have
436 separated into the counterpart of the sample during preparation.

437

438 Figure 2. SEMs of vertical sections through the fossil skin showing variation in the relative
439 abundance of different chromatophores (A–C, G–I) with interpretative drawings (D–F, J–L).
440 Encircled numerals correspond to sample numbers in Figure 1(A). (A) Abundant xanthophores,
441 common iridophores and melanophores. Epi., epidermis. (B) Common iridophores and
442 xanthophores, occasional melanophores. (C) Abundant iridophores, common melanophores and
443 xanthophores. (G) Abundant melanophores, common xanthophores, rare iridophores. (H)
444 Abundant xanthophores, occasional iridophores, rare melanophores. (I) Abundant xanthophores
445 and iridophores, rare melanophores. See also Figures S1–S4.

446

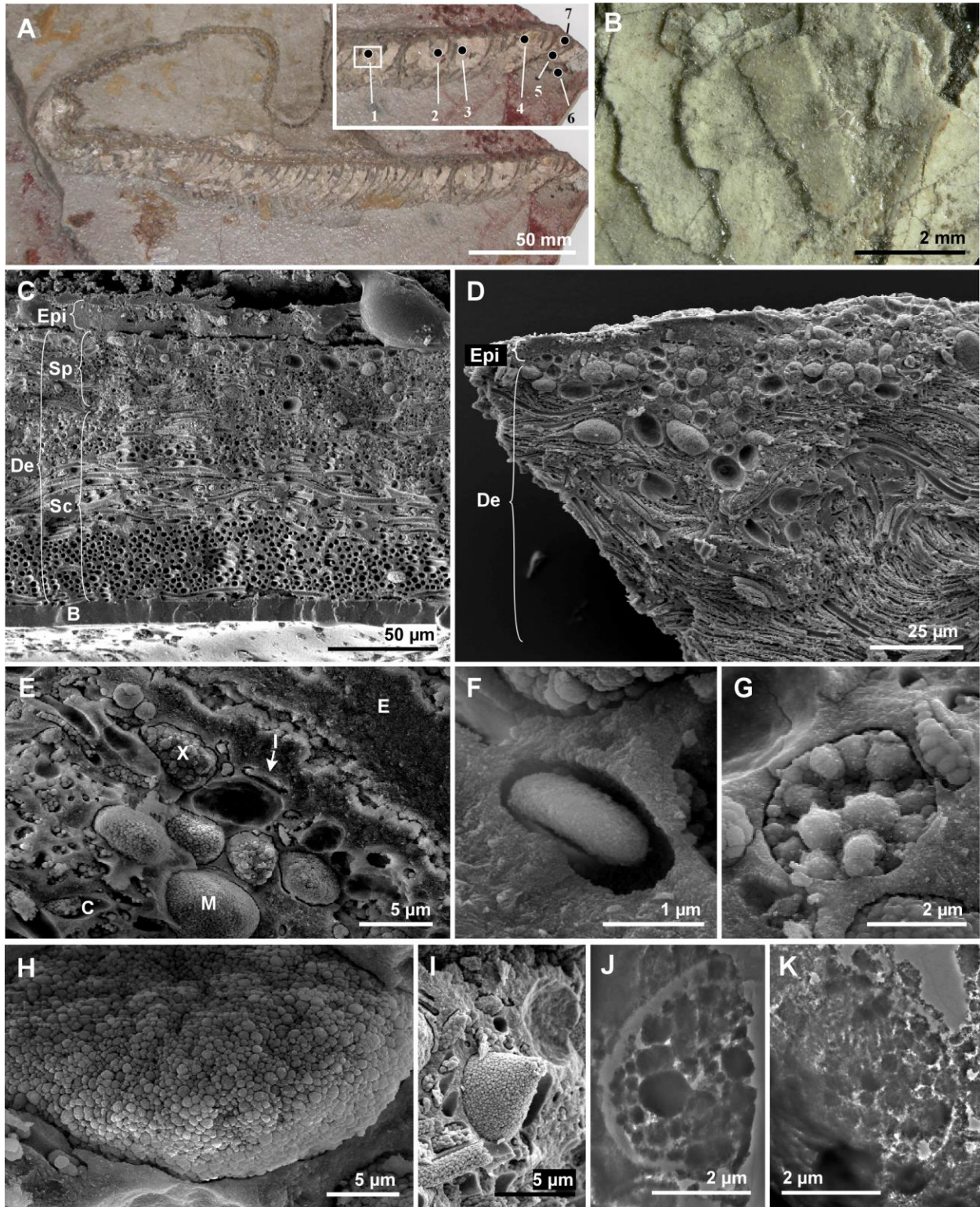
447 Figure 3. Electron probe microanalysis X-ray maps of a polished vertical section through the
448 skin of the fossil snake MNCN 66503. Areas mapped in (A) and (B) show the uppermost stratum
449 spongiosum; the upper surface of the skin is to the left in (A) and associated elemental maps for
450 C, Mg, Al, P, S, Cl, K, Ca, Mn, Fe and Cs, and to the top of (B) and associated maps for Co, Cu

451 and Zn. C, collagen fibre; M, melanophore; X, xanthophore. Limited variation in tone in maps
452 for Cu, Co and Zn indicate consistently low concentrations of these elements over the area
453 analyzed; colour scale for all other images ranges from blue (low values) to red (high values).
454 Scale bars: 10 μm .

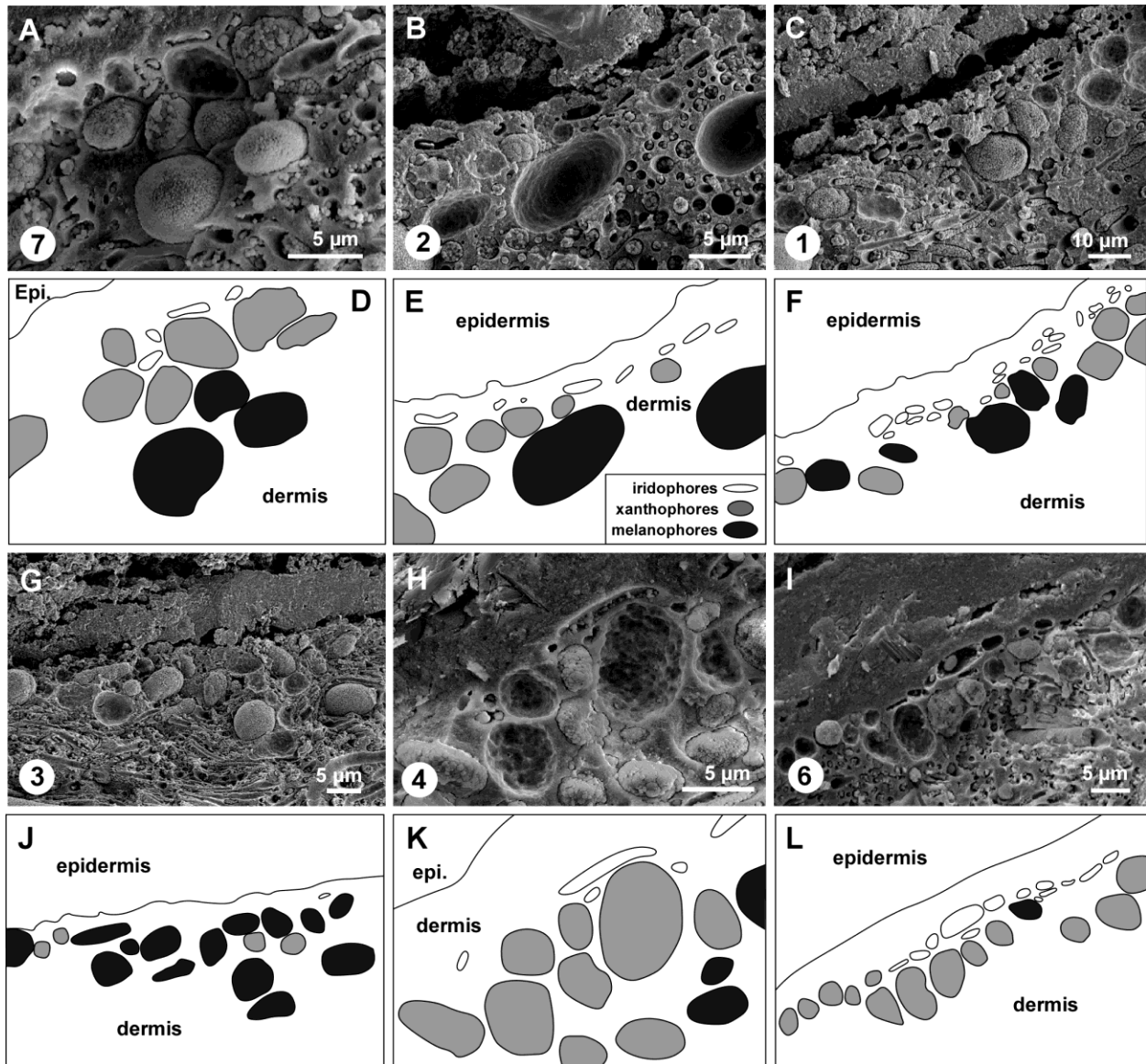
455

456 Figure 4. Colour reconstruction of the fossil snake MNCN 66503. (A) Schematic representation
457 of the relative abundance and position of chromatophores in samples of skin from different body
458 regions. Numbers denote samples discussed in the text. See also Tables S1, S2. (B) Colour plate
459 is by Jim Robbins.

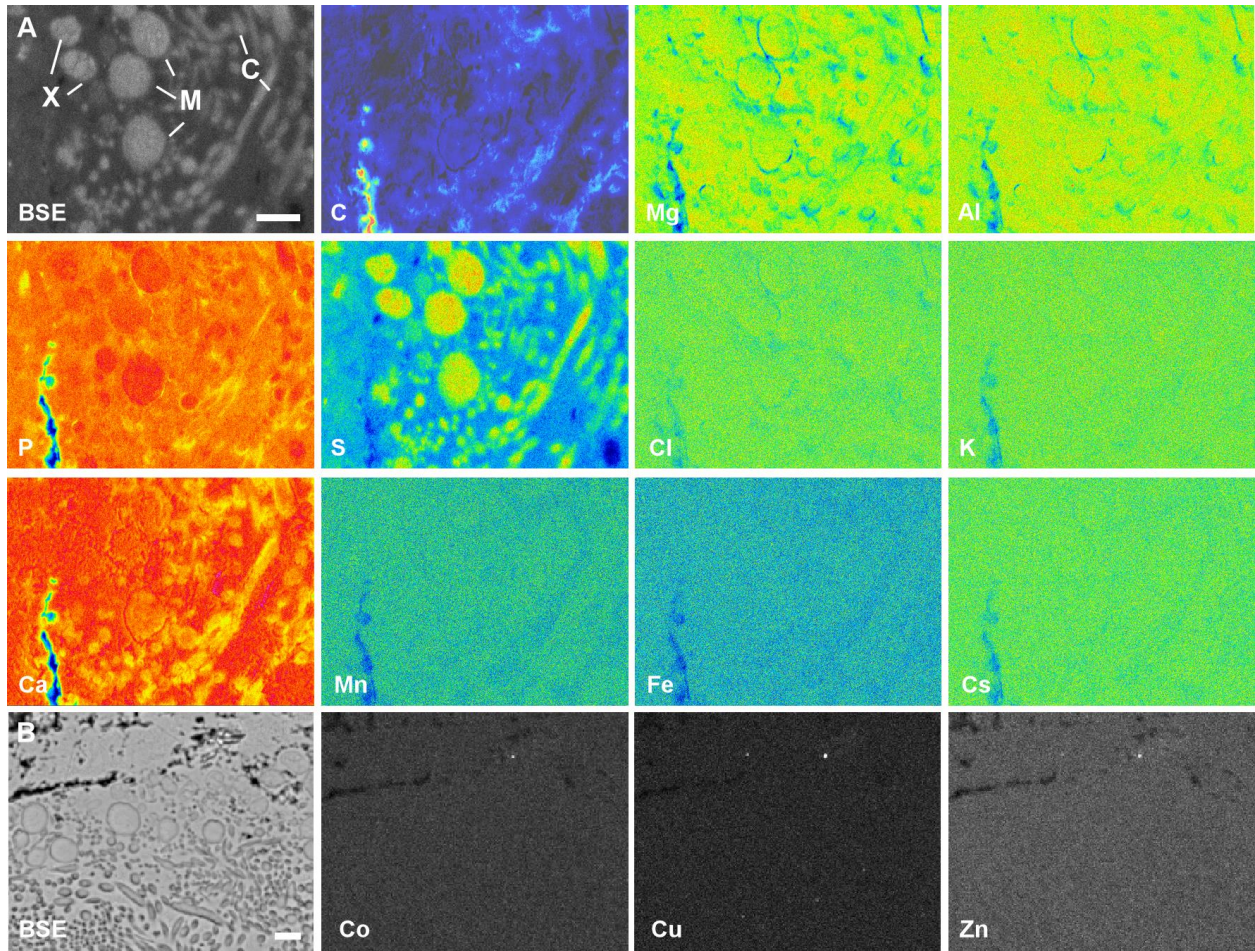
460



McNamara et al. Figure 1



McNamara et al. Figure 2



McNamara et al. Figure 3

463

464